Geophysical Research Letters

RESEARCH LETTER
10.1029/2021GL092722

Stable Atlantic Deep Water Mass Sourcing on Glacial-Interglacial Timescales

Frerk Pöppelmeier[1,2], Marcus Gutjahr[3], Patrick Blaser[2,4], Hartmut Schulz[5], Finn Süfke[2], and Jörg Lippold[2]

[1]Climate and Environmental Physics, Physics Institute and Oeschger Center for Climate Change Research, University of Bern, Bern, Switzerland, [2]Institute of Earth Sciences, Heidelberg University, Heidelberg, Germany, [3]GEOMAR Helmholtz Center for Ocean Research Kiel, Kiel, Germany, [4]Institute of Earth Sciences, University of Lausanne, Lausanne, Switzerland, [5]Institute of Earth Sciences, University of Tübingen, Tübingen, Germany

Key Points:

- New authigenic εNd record of North Atlantic site U1313 covering the past ~100 kyr reflects northern end-member variations
- Northern and southern εNd end-members largely evolved in tandem during the last glacial cycle
- High proportions of northern-sourced water dominated the Atlantic throughout the past 100 kyr, culminating during Marine Isotope Stage 4

Supporting Information:

Supporting Information may be found in the online version of this article.

Correspondence to:

F. Pöppelmeier,
frerk.poeppelmeier@climate.unibe.ch

Citation:

Pöppelmeier, F., Gutjahr, M., Blaser, P., Schulz, H., Süfke, F., & Lippold, J. (2021). Stable Atlantic deep water mass sourcing on glacial-interglacial timescales. *Geophysical Research Letters*, *48*, e2021GL092722. https://doi.org/10.1029/2021GL092722

Received 29 JAN 2021
Accepted 1 JUL 2021

Abstract Increased deep ocean carbon storage is often invoked as the major sink for lower atmospheric CO_2 concentrations during past ice ages. In order to improve the understanding of the changes in ocean dynamics facilitating such increased oceanic carbon storage, we assess the variability of deep water provenance in the Atlantic by reconstructing authigenic Nd isotopes from North Atlantic site U1313 over the past ~100 kyr. Under consideration of these new constraints for the northern Nd isotope end-member, we find only limited long-term variations in the meridional and intra-basin water-mass gradients suggesting a prevalence of northern-sourced water (NSW) throughout the past 100 kyr. Tentative results suggest that during the glacial period of Marine Isotope Stage 4 NSW proportions even increased by additional ~15% in the equatorial and Northeast Atlantic, calling into question the notion that cold climates promote the expansion of southern-sourced water.

Plain Language Summary The deep ocean is the largest carbon reservoir that can take up or release CO_2 on short timescales. In order to improve predictions of potential carbon transfer from the atmosphere to the deep sea, it is therefore central to understand the processes that facilitate increased ocean carbon storage. Here we investigate the Atlantic deep ocean water mass structure over the last 100,000 years, during which atmospheric CO_2 concentrations slowly decreased by about 100 ppm until the peak of the last ice age 20,000 years ago. Our new reconstructions indicate a remarkably stable Atlantic deep water mass structure during that time. This finding contrasts previous investigations that suggested expansion of southern-sourced water with colder climates. We here argue that changes in the physico-chemical properties in the deep water source regions can explain the intra-basin changes on which previous inferences of southern-sourced water expansion were based on. If confirmed, this suggests that the increased oceanic carbon storage during the last ice age was not a result of changes in deep water mass structure in the Atlantic. Instead, it seemed to be more closely related to changes in deep water transport rates, recycling of biological material, and/or changes associated with increased sea-ice extent.

1. Introduction

The last glacial period (~110–~18 kyr Before Present (BP)) was characterized by gradually decreasing atmospheric CO_2 concentrations mainly responsible for the decreasing global temperatures that culminated in the Last Glacial Maximum (LGM) (Bereiter et al., 2012). Overall, atmospheric CO_2 concentrations declined by about 100 ppm during the last glacial cycle (Petit et al., 1999). The majority of this carbon must have been stored away in the deep oceans, which constitute the largest carbon reservoir able to readily take up and release CO_2 (Broecker, 1982; Rahmstorf, 2002). In light of this, it was speculated that both long-lasting changes and short-term oscillations in global climate during the last glacial cycle were linked to changes in the strength and geometry of the Atlantic Meridional Overturning Circulation (AMOC; Curry & Oppo, 2005; McManus et al., 2004). However, reconstructions of conservative water mass tracers covering the entire last glacial cycle are arguably very sparse and as such the variability of the AMOC during this time period remains poorly constrained.

Here we use neodymium (Nd) isotopes extracted from sedimentary authigenic Fe-Mn oxyhydroxides to reconstruct the water mass provenance and mixing between northern- and southern-sourced deep water

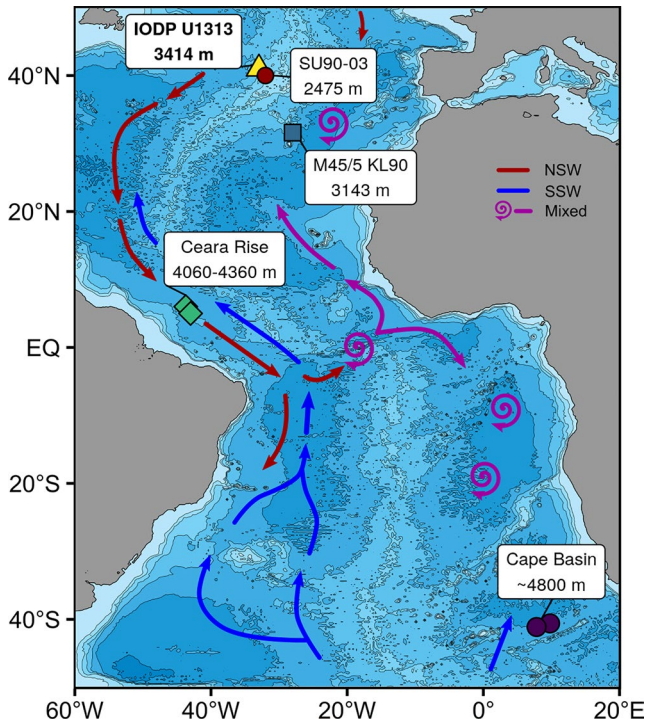

Figure 1. Modern hydrography and site locations. New εNd data from site U1313 are compared to records from M45/5 KL90 (Pöppelmeier, Frank, et al., 2020), SU90-03 (Howe, Piotrowski, Noble, et al., 2016), the Ceara Rise (ODP 929, Howe & Piotrowski, 2017; EW9209-1, Curry & Oppo, 1997) and the composite of two sites from the Cape Basin (RC11-83 and TN057-21 (Piotrowski et al., 2004, 2005)). Blue and red arrows indicate southern sourced water (SSW) and northern sourced water (NSW), respectively. Purple arrows mark mixtures of NSW and SSW, with spirals indicating areas of strongly mixed deep water.

masses (NSW and SSW, respectively). Archived authigenic phases are found to faithfully record the local bottom water Nd isotopic signature of pelagic sediments in the Atlantic (e.g., Blaser et al., 2016; Tachikawa et al., 2017). The Nd isotope water mass tracer is independent of biological processes and thus allows for disentangling changes in AMOC geometry from variations in carbon cycling. In the modern Atlantic NSW has a Nd isotope signature (denoted as εNd, which is $^{143}Nd/^{144}Nd$ relative to the Chondritic Uniform Reservoir (Jacobsen & Wasserburg, 1980) per 10,000) of around −13 (Lambelet et al., 2016) while SSW exhibits more radiogenic signatures of about −9 (Stichel et al., 2012). However, it has been shown that these end-member values are variable on glacial-interglacial timescales presumably due to changes in the high-latitude weathering regimes modulating the Nd input into the oceans (Zhao et al., 2019) as well as changes in the location of deep water formation (Huang et al., 2020). As such, it is crucial to constrain the εNd end-member characteristics throughout the last glacial cycle before any meaningful interpretation of intra-basin water mass mixing based on Nd isotopes can be achieved for this time period. Reconstruction of the southern end-member from an εNd record of the abyssal Southeast Atlantic Cape Basin (~4,800 m water depth; Figure 1), indicates glacial-interglacial changes over the last glacial cycle of about 3 ε-units (between −9.5 and −6.5, Piotrowski et al., 2005) with changes up to ~4 ε-units observed at the Mid-Atlantic Ridge during Termination 1 (MAR, Skinner et al., 2013). In contrast, high-resolution end-member constraints for NSW exist only for the past 20 kyr, but indicate variability of similar magnitude as observed in the South Atlantic ($\Delta\varepsilon Nd \approx 3.5$, between −14.0 and −10.5; Zhao et al., 2019). Here we reconstructed the Nd isotopic composition of IODP site U1313 (Figure 1) over the past 100 kyr and build the case that this site was never bathed by significant proportions of SSW during the entire investigated timespan, which recent studies already indicated for the LGM (Du et al., 2020; Pöppelmeier, Blaser, et al., 2020). Hence, U1313 is considered representative of NSW end-member variations over the last glacial cycle. With these new end-member constraints at hand, we then evaluate the water mass provenance and mixing at the equatorial Atlantic as well as the intra-basin water mass exchange between the East- and West Atlantic over the past ~100 kyr.

2. Materials and Methods

2.1. Sediment Core

IODP site U1313 (Leg 306) is a reoccupation of DSDP site 607 located on the western flank of the MAR (41.00°N, 32.96°W) at 3,414 m water depth (Channell et al., 2006). The chronostratigraphy of site U1313 was previously established by Naafs et al. (2013) based on correlation of sedimentary features (quartz/calcite, and dolomite/calcite ratios) with the proximate and well-dated sediment core U1308 as well as planktic $\delta^{18}O$ correlations to the LR04 stack (Smith et al., 2013). The average sedimentation rate of the here investigated interval is ~5.4 cm/kyr. Site U1313 is purely bathed by North Atlantic Deep Water (NADW) in the modern ocean.

2.2. Sample Preparation and Measurement

Authigenic Fe-Mn oxyhydroxide-derived Nd was extracted from bulk sediment following the leaching protocol by Blaser et al. (2016), which has proven to reliably extract the authigenic phase in very good agreement with other archives (e.g., Huang et al., 2020; Pöppelmeier et al., 2018, 2019, Figure S2). Nd was separated from the sample matrix by a two-step column chromatography with 50W-X8 and Ln-Spec resins. Nd isotopes were analyzed on two Neptune Plus MC-ICP-MS at GEOMAR, Kiel and Heidelberg

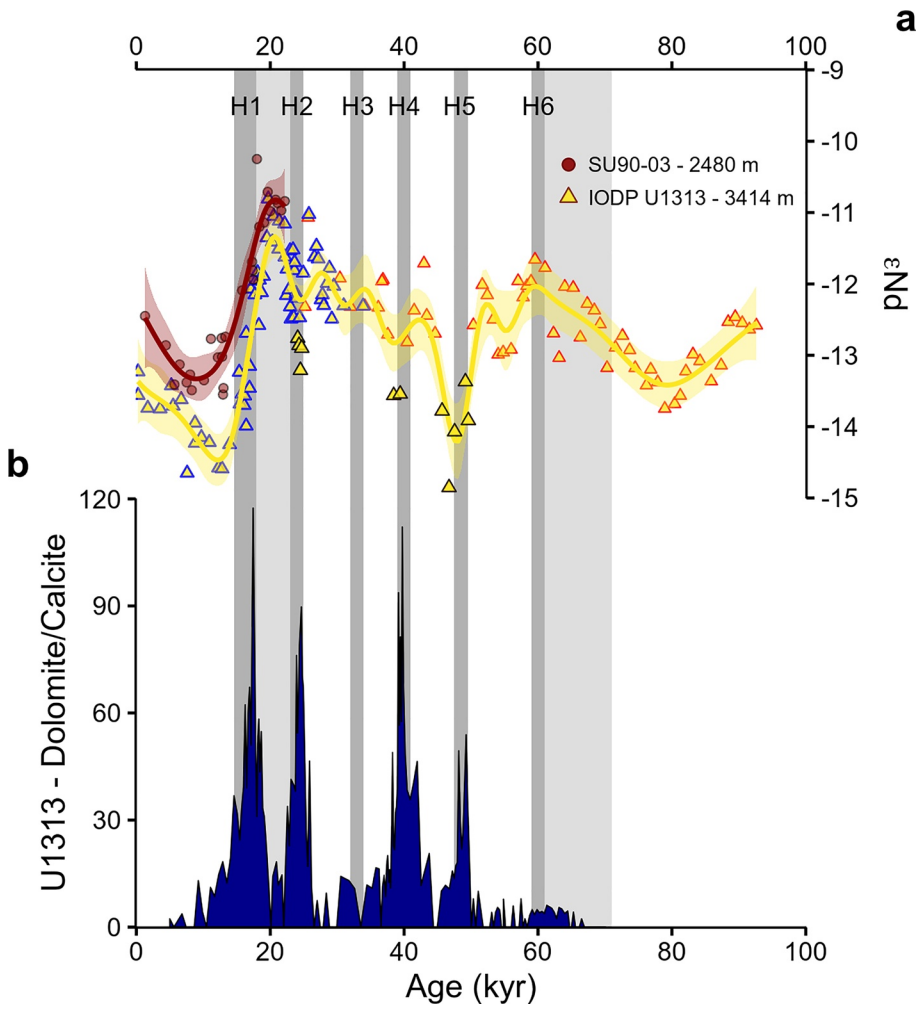

Figure 2. (a) Composite of all published (blue borders, Lang et al., 2016; Lippold et al., 2016; Pöppelmeier et al., 2018) and new εNd data of site U1313 in comparison to εNd data from SU90-03 (Howe, Piotrowski, Noble, et al., 2016) about 1,000 m shallower than U1313 (Figure 1). U1313 data with black borders reflect samples affected by in situ alterations caused by detrital carbonates during major Heinrich events. (b) dolomite/calcite ratios, which only extend back to 70 kyr BP (Naafs et al., 2013).

University. Isotope measurements were corrected for instrumental mass bias by normalizing $^{146}Nd/^{144}Nd$ to 0.7219 using an exponential mass fractionation correction. Samples were further bracketed by concentration-matched JNdi-1 standard solutions corrected to the accepted value of $^{143}Nd/^{144}Nd = 0.512115$ (Tanaka et al., 2000). The external reproducibility (2SD) was determined by repeated measurements of secondary in-house standards varying between 0.18 and 0.45 ε-units. Total procedural blanks were always below 0.1% of sample Nd concentrations and are thus negligible.

3. Results

The new Nd isotope data of site U1313 complement previously published reconstructions (Lang et al., 2016; Lippold et al., 2016; Pöppelmeier et al., 2018) back to ~95 kyr BP (Figure 2a). The published and new data extracted from different archives (fish debris, strong and weak reductive sediment leaches) overlapping in the time range between 25 and 35 kyr BP agree well (Figure S2), providing confidence in the veracity of the extracted signal to represent the local authigenic Nd isotope signatures. The most radiogenic (high) values are observed during the LGM and the late Marine Isotope Stage 4 (MIS4). Unradiogenic excursions at ~26,

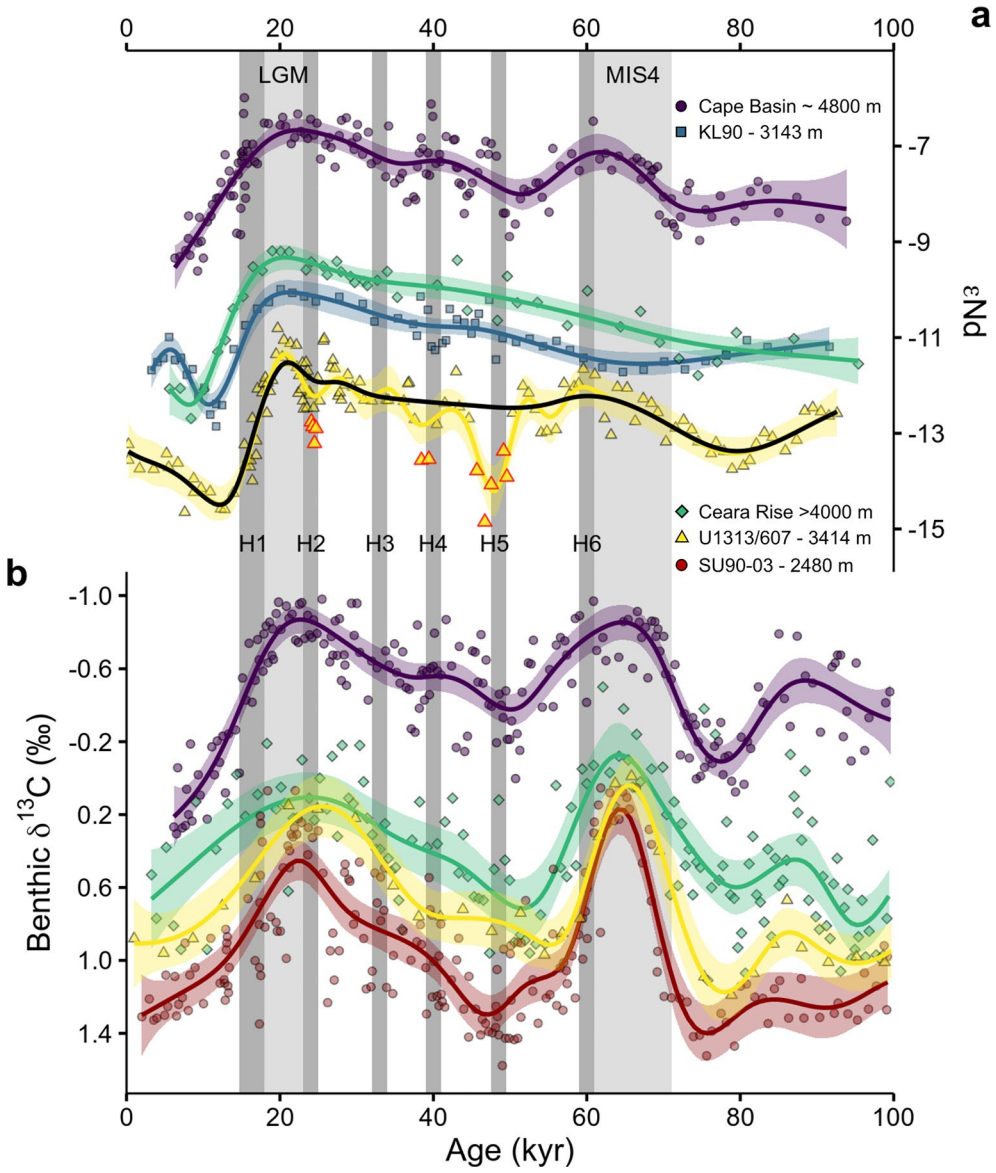

Figure 3. (a) Nd isotope records from the deep Atlantic covering the past 100 kyr. The Cape Basin record is a composite of sites RC11-83 (Piotrowski et al., 2004) and TNO57-21 (Piotrowski et al., 2005). Site U1313 data (past 35 kyr: Lang et al., 2016; Lippold et al., 2016; Pöppelmeier et al., 2018) are complemented by new data back to ~95 kyr BP. Data of ODP 929 and M45/5 KL90 are from Howe and Piotrowski (2017) and Pöppelmeier, Frank et al. (2020), respectively. U1313 data with red borders were excluded for the black line fit due to in situ alterations by detrital carbonate during major Heinrich events. (b) Bottom water stable carbon isotope data ($\delta^{13}C$) of the Cape Basin (TNO57-21, Charles et al., 1996), Ceara Rise (EW9209-1, 4,056 m water depth, proximal to ODP 929, Curry & Oppo, 1997; Figure S3), DSDP 607 (Ruddiman et al., 1989, with refined age model cf. Figure S4), and SU90-03 (Chapman et al., 2000). Lines with error bands (95% confidence interval) represent fits with a generalized additive model.

~40, and ~50 kyr BP coincide with dolomite/calcite peaks associated with detrital carbonate input by iceberg rafting during Heinrich events 2, 4, and 5, respectively (Figure 2c).

The core-top Nd isotope signature of site M45/5 KL90 (−11.7 ± 0.13, hereafter KL90, Text S1) is in good agreement with nearby seawater data (−11.4 to −11.8, Station 5 of Stichel et al., 2015), again corroborating the reliability of the method to extract the local bottom water signature. Due to the low sedimentation rate of site KL90 millennial-scale variations cannot be resolved in this core. The overall εNd evolution throughout the last glacial cycle mirrors the record of the equatorial site ODP 929 (Figure 3, Howe & Piotrowski, 2017)

but with slightly less radiogenic values (0.50–0.75 ε-units) from 80 kyr BP onward. The least radiogenic values are observed during the early Holocene similar to most Atlantic εNd records (Pöppelmeier, Scheen, et al., 2020).

4. Discussion

Nutrient-based reconstructions of the LGM water mass structure suggest a considerably shallower boundary between NSW and SSW with lower benthic stable carbon isotope signatures ($\delta^{13}C$) in the deep North Atlantic as a result of reduced NSW contribution (e.g., Curry & Oppo, 2005). A potentially shallower glacial water mass boundary could question the reliability of site U1313 to represent the NSW end-member characteristics, as SSW could have contributed to the local bottom water under such conditions. Recent investigations of the glacial AMOC geometry based on Nd isotopes, however, provide evidence that the overall water mass distribution during the LGM was similar to the modern ocean (Du et al., 2020; Howe, Piotrowski, Noble, et al., 2016; Pöppelmeier, Blaser, et al., 2020). Revised evaluations of LGM nutrient-based reconstructions further indicate minimal influence of SSW north of 40°N (Gebbie, 2014; Oppo et al., 2018). Moreover, the concurrent evolution of the εNd (Figure 2a) as well as $\delta^{13}C$ (Figure 3b) records of sites U1313 and SU90-03, that is, situated near U1313 but about 1 km shallower (Figure 1), strongly supports the reliability of U1313 to represent the northern end-member. This is based on the rationale that the shallower SU90-03 is expected to have been bathed by nearly pure NSW at all times, and hence the close resemblance of the εNd and $\delta^{13}C$ records of both sites indicates that this also holds true for U1313. The slight difference between both Nd isotope records with less radiogenic values of U1313 during the early Holocene can be attributed to the well investigated unradiogenic Nd input into the Labrador Sea (Howe, Piotrowski, & Rennie, 2016; Pöppelmeier et al., 2019, Pöppelmeier, Scheen, et al., 2020). This input is thought to have mainly influenced the bottom water Nd isotope signatures of the entire Atlantic with diminishing effect at shallower depths. While we cannot fully exclude the impact of such process further downcore, the unradiogenic Nd input potentially offsetting the record toward lower signatures would render U1313 as the unradiogenic lower limit of the northern εNd end-member. Thus, mixing calculations would slightly underestimate the NSW fraction. In addition, Zhao et al. (2019) recently reported εNd end-member variations of NSW since the LGM in agreement with the glacial-interglacial shift of U1313 again lending support to U1313 representing the Nd isotope end-member of deep NSW (Figure S2). Finally, the northward expansion of SSW is suggested to have peaked during the LGM (Lynch-Stieglitz et al., 2007) for which we however find no indication of significant SSW contribution at U1313 as laid out above. From this and the parallel evolution of the U1313 and SU90-03 $\delta^{13}C$ records over the past 100 kyr we infer that site U1313 was also not influenced by significant amounts of SSW prior to the LGM. This corroborates the findings by Jaume-Seguí et al. (2020), who identified U1313 to represent the northern end-member also throughout the mid-Pleistocene.

Site U1313 is situated at the southern boundary of the ice rafted debris belt and as such the sediments deposited during major Heinrich events (H1, H2, H4, and H5) are enriched in Laurentian detrital carbonate (Figure 2c; Naafs et al., 2013). Detrital carbonate derived from the Canadian Shield exhibits exceptionally unradiogenic Nd isotope signatures (<-20; Grousset et al., 2001) and early diagenesis can lead to incorporation of this signature in the authigenic signal, which has the potential to overprint the local bottom water authigenic Nd isotope signatures (Blaser et al., 2019). However, this detrital overprinting has been shown to be strictly limited to the Heinrich layers and does not affect the adjacent sediment (Blaser et al., 2019). Therefore, we argue that unradiogenic εNd excursions of site U1313 during H2, H4, and H5 result from in situ detrital overprinting and do not reflect actual bottom water Nd isotope signature changes. We thus exclude these data points from further paleoceanographic interpretations (Figure 3). The same process may have contributed to the decreasing trend in εNd during H1, but we are unable to disentangle the potential detrital overprinting from deglacial AMOC reorganizations during that time. A recent study suggests detrital overprinting to be relevant also during H1 (Du et al., 2020). Thus, we here focus on the glacial evolution of the AMOC and only to a lesser extent on the last deglaciation.

In order to derive the proportion of NSW bathing the equatorial and the Northeast Atlantic, we apply a binary mixing model to the εNd records of ODP 929 (Howe & Piotrowski, 2017) and KL90 (Pöppelmeier, Frank, et al., 2020). Both sites are predominantly bathed by NSW in the modern ocean with minor contributions of SSW. For these calculations we define the northern and southern end-member variations by the εNd

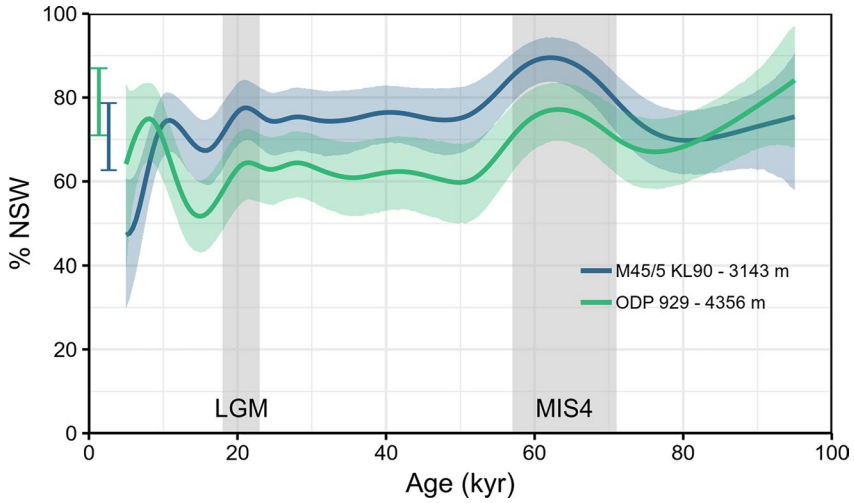

Figure 4. Proportions of northern sourced water (NSW) at sites KL90 (Pöppelmeier, Frank, et al., 2020) and ODP 929 (Howe & Piotrowski, 2017) derived from a binary mixing model assuming U1313 and the Cape Basin composite as northern and southern end-members, respectively. Uncertainties are propagated with a Monte-Carlo approach from the confidence intervals of the end-member records as well as KL90/ODP 929. The uncertainty of the Nd concentration end-members are estimated to ±10% and are also incorporated in the Monte-Carlo error propagation. Modern %NSW based on conservative water mass properties (Jenkins et al., 2015; Pöppelmeier, Blaser, et al., 2020) are marked on the left.

reconstructions of site U1313 and the Cape Basin composite (Figure 3a), respectively. Both end-member sites exhibit substantially higher sedimentation rates than ODP 929 and KL90 and hence resolve millennial-scale variability that is, smoothed out by bioturbation and the lower temporal sampling resolution of the ODP 929 and KL90 records. Therefore, we extract the long-term trends by applying generalized additive models (Simpson, 2018), that limit the degrees of freedom of the fits (i.e., we under-fit the high-resolution data to only represent the long-term trends). We note here that the Cape Basin composite record may not be fully representative of the southern εNd end-member at all times as indicated by the differences during the LGM to a proximate record from the MAR (Skinner et al., 2013) and recent reports of benthic modification of bottom water εNd with a less radiogenic signature (−10.0 ± 0.5; Rahlf et al., 2020), which would lead to a slight underestimation of the NSW contribution. Yet, no other εNd record of the South Atlantic/Southern Ocean exists that covers the entire last 100 kyr. Further, no proxy and hence no information on past Nd concentrations is available, for that reason we use modern values for NSW (18 pmol/kg; Lambelet et al., 2016) and SSW (27 pmol/kg; Stichel et al., 2012) in the binary mixing calculations. In order to account for these missing constraints, we consider an additional uncertainty of ±10% of the end-member Nd concentrations in the Monte-Carlo error propagation for the uncertainty of the mixing calculations (Figure 4).

Based on these Nd isotope mixing calculations both ODP 929 and KL90 were dominated by NSW throughout the past 100 kyr with absolute proportions of at least 60% (±10%), and a maximum of 90% (±5%) NSW at site ODP 929 during MIS4 (Figure 4). Analogous calculations based on $\delta^{13}C$ yield similar results (Figure S5) corroborating this εNd-based approach for deriving past NSW proportions. Minimum NSW contributions are observed during the deglaciation for KL90 and early Holocene for ODP 929. Whether these deglacial variations truly reflect changes in water mass sourcing is questionable, since the εNd end-member constraint from U1313 may have been compromised by detrital carbonate during H1 as mentioned above. Further, the Holocene variations in NSW contribution of KL90 are potentially biased by the limited age constraints of that core. Nevertheless, the overall meridional as well as intra-basin water mass distribution of the Atlantic seems to have been mostly invariant to shifts in the long-term climatic boundary conditions. The relatively stable water mass provenance at sites ODP 929 and KL90, in spite of substantial variations in local εNd, can be attributed to the parallel evolutions of the northern and southern εNd end-member records, which indeed follow long-term climatic variations. The northern Nd isotope end-member seems to be largely

controlled by the extent of the Laurentide ice-sheet limiting the influx of unradiogenic Nd from the Canadian Shield during glacial conditions (Blaser et al., 2020; Zhao et al., 2019) or shifts in deep water formation regions (Du et al., 2020) producing a more radiogenic northern end-member as observed in particular during the LGM and MIS4. Contrastingly, the mechanisms responsible for the southern εNd end-member variations are less clear. Huang et al. (2020) found first indications for the absence of unradiogenic Weddell Sea bottom water formation during glacial maxima, which, in the modern ocean, contributes to the SSW entering the Atlantic. In addition, NSW ultimately feeds into SSW via lower circumpolar deep water and hence any end-member shift of NSW is propagated into SSW, although the signal amplitude is strongly attenuated by mixing with various other water masses in the Southern Ocean (van de Flierdt et al., 2016). As such, a multitude of factors that are difficult to disentangle control the southern εNd end-member.

While the εNd records from U1313 and the Cape Basin evolve largely in tandem throughout the past 100 kyr, both ODP 929 and KL90 do not follow the same trend as the end-members during MIS4. Even though the temporal resolutions of ODP 929 and KL90 are arguably low, a trend toward more radiogenic εNd over the more than 10 kyr lasting MIS4 should be resolvable at least for KL90. Thus, it appears that NSW slightly expanded southward during glacial MIS4, contradictory to the prevailing notion that SSW expands under colder climate conditions (e.g., Lynch-Stieglitz et al., 2007).

The new finding of relatively stable water mass sourcing throughout the last glacial cycle contrasts previous studies reporting substantial shoaling of NSW during cold climate periods mainly inferred from $\delta^{13}C$ (e.g., Curry & Oppo, 2005; Lynch-Stieglitz et al., 2007). However, benthic $\delta^{13}C$ from the North to South Atlantic also evolved largely in parallel over the past 100 kyr (Figure 3b). This is commonly interpreted as an expansion of SSW even into the high latitude North Atlantic during glacial maxima. Yet, this hypothesis is not supported by the new Nd isotope data presented here indicating no significant SSW contributions at U1313 even during the LGM. No significant presence of SSW at U1313 is further corroborated by the close correlation of the $\delta^{13}C$ records (similar to εNd) of U1313 and the 1 km shallower SU90-03 throughout the past 100 kyr. The locations of U1313 and SU90-03 in the North Atlantic between 2.5 and 3.5 km water depth make them ideally situated to trace the evolution of a potential NSW shoaling, which is expected to lower $\delta^{13}C$ of U1313 to a greater extent than at SU90-03. However, diverging $\delta^{13}C$ records of U1313 and SU90-03 during glacial maxima are not observed (Figure 3b). In fact, both records even slightly converge during the LGM and MIS4. These data therefore suggest that the large glacial-interglacial $\delta^{13}C$ swings of up to 1‰ were not dominated by changes in water mass mixing but instead were presumably more closely related to changes in $\delta^{13}C$ end-member properties. The well-established lower glacial end-member of the Southern Ocean is thought to be related to larger air-sea gas disequilibrium due to greater sea-ice extent (Marchitto & Broecker, 2006) and enhanced export productivity fueled by iron fertilization from elevated dust fluxes ($\delta^{13}C$ of respired organic matter ∼−20‰, Jaccard et al., 2016). These processes could have also played an important role in lowering the northern $\delta^{13}C$ end-member signature, yet more research is required regarding this hypothesis. The notion that end-member variations were mainly responsible for the large $\delta^{13}C$ swings is further substantiated by $\delta^{13}C$ records at the equatorial Ceara Rise (sites ODP 929 and EW9202-1; Figure 3 and Figure S3), which evolved very similarly to the North Atlantic records. Nearly during the entire past 100 kyr, the meridional $\delta^{13}C$ gradient was smaller in the North Atlantic (difference Ceara Rise to U1313/SU90-03) than the South Atlantic (difference Ceara Rise to Cape Basin). This asymmetry in the meridional gradient was most pronounced during MIS4 and the LGM, when the deep equatorial and North Atlantic sites recorded almost equal $\delta^{13}C$ signatures. Such a gradient is reminiscent of the modern hydrography, but is difficult to explain with expanded SSW.

Recent evidence for the close resemblance between modern and LGM water mass sourcing featuring expansive NSW (Du et al., 2020; Howe, Piotrowski, Noble, et al., 2016; Pöppelmeier, Blaser, et al., 2020), and the qualitative agreement between εNd and $\delta^{13}C$ reconstructions laid out above support the notion that colder climates do not necessarily lead to a reduction of NSW proportion in the Atlantic. However, we note that the here presented results do not exclude centennial to millennial-scale variations of water mass provenance thought to be central to Dansgaard-Oeschger cycles (e.g., Menviel et al., 2014). The sedimentation rates of the εNd records do not permit to resolve such features.

5. Conclusions

We presented new authigenic εNd data of North Atlantic site U1313. Supported by a comparison to the shallower site SU90-03, it is demonstrated that site U1313 was not bathed by significant amounts of SSW over the past 100 kyr, and hence faithfully represents the northern εNd end-member. Combining these new northern Nd isotope end-member constraints with previously published εNd reconstructions from the Southeast Atlantic Cape Basin, representing the southern end-member, a binary mixing calculation suggests high proportions of NSW bathing the equatorial and Northeast Atlantic continuously since the initiation of the last glaciation. This is largely attributed to the concurrent evolutions of both end-members as well as the intra-basin records over the past ~100 kyr, generally exhibiting more radiogenic signatures during colder climates and less radiogenic ones during warm periods. The only major exception is glacial MIS4 when NSW contributions at both intra-basin sites appear to have been ~15% higher than the baseline during the last glacial cycle. These findings are corroborated by $\delta^{13}C$ records from the same locations also evolving predominantly in tandem over the past 100 kyr indicating similar large and concurrent glacial-interglacial swings in end-member compositions. Hence, this result contradicts the notion that colder climates promoted the expansion of SSW in the deep Atlantic. If confirmed, this suggests that the increased glacial carbon storage was not a result of changes in deep ocean water mass provenance in the Atlantic but instead was more closely related to (more sluggish) deep ocean advection, enhanced export productivity, and/or changes in air-sea gas exchange/disequilibrium due to increased sea-ice extent.

Data Availability Statement

Data of this study can be found in the supporting information, at http://doi.org/10.5281/zenodo.4705368, and at PANGAEA (https://doi.pangaea.de/10.1594/PANGAEA.932768).

Acknowledgments
The authors thank the IODP core repository Bremen for providing sample material. Norbert Frank and Sönke Szidat are thanked for analytical support. This study was made possible by grant Li1815/9-1 of the German Research Foundation (DFG). P. Blaser, F. Süfke, and J. Lippold are supported by the Emmy-Noether Program of the German Research Foundation (grant Li1815/4). The authors further thank two reviewers for particularly helpful comments. Open access funding enabled and organized by Projekt DEAL.

References

Bereiter, B., Lüthi, D., Siegrist, M., Schüpbach, S., Stocker, T. F., & Fischer, H. (2012). Mode change of millennial CO_2 variability during the last glacial cycle associated with a bipolar marine carbon seesaw. *Proceedings of the National Academy of Sciences*, *109*(25), 9755–9760. https://doi.org/10.1073/pnas.1204069109

Blaser, P., Gutjahr, M., Pöppelmeier, F., Frank, M., Kaboth-Bahr, S., & Lippold, J. (2020). Labrador sea bottom water provenance and REE exchange during the past 35,000 years. *Earth and Planetary Science Letters*, *542*, 116299. https://doi.org/10.1016/j.epsl.2020.116299

Blaser, P., Lippold, J., Gutjahr, M., Frank, N., Link, J. M., & Frank, M. (2016). Extracting foraminiferal seawater Nd isotope signatures from bulk deep sea sediment by chemical leaching. *Chemical Geology*, *439*, 189–204. https://doi.org/10.1016/j.chemgeo.2016.06.024

Blaser, P., Pöppelmeier, F., Schulz, H., Gutjahr, M., Frank, M., Lippold, J., et al. (2019). The resilience and sensitivity of Northeast Atlantic deep water εNd to overprinting by detrital fluxes over the past 30,000 years. *Geochimica et Cosmochimica Acta*, *245*, 79–97. https://doi.org/10.1016/j.gca.2018.10.018

Broecker, W. S. (1982). Glacial to interglacial changes in ocean chemistry. *Progress in Oceanography*, *11*(2), 151–197. https://doi.org/10.1016/0079-6611(82)90007-6

Channell, J. E. T., Sato, T., Stein, R., Alvarez Zarikian, C. A., Malone, M. J., & the Expedition 303/306 Scientists (2006). *Proceedings of IODP*. Integrated Ocean Drilling Program Management International, Inc. https://doi.org/10.2204/iodp.proc.303306.112.2006

Chapman, M. R., Shackleton, N. J., & Duplessy, J. C. (2000). Sea surface temperature variability during the last glacial-interglacial cycle: Assessing the magnitude and pattern of climate change in the North Atlantic. *Palaeogeography, Palaeoclimatology, Palaeoecology*, *157*(1–2), 1–25. https://doi.org/10.1016/S0031-0182(99)00168-6

Charles, C. D., Lynch-Stieglitz, J., Ninnemann, U. S., & Fairbanks, R. G. (1996). Climate connections between the hemisphere revealed by deep sea sediment core/ice core correlations. *Earth and Planetary Science Letters*, *142*, 19–27. https://doi.org/10.1016/0012-821X(96)00083-0

Curry, W. B., & Oppo, D. W. (1997). Synchronous, high-frequency oscillations in tropical sea surface temperatures and North Atlantic deep water production during the last glacial cycle. *Paleoceanography*, *12*(1), 1–14. https://doi.org/10.1029/96PA02413

Curry, W. B., & Oppo, D. W. (2005). Glacial water mass geometry and the distribution of $\delta^{13}C$ of ΣCO_2 in the western Atlantic Ocean. *Paleoceanography*, *20*(1), PA1017. https://doi.org/10.1029/2004PA001021

Du, J., Haley, B. A., & Mix, A. C. (2020). Evolution of the global overturning circulation since the last glacial maximum based on marine authigenic neodymium isotopes. *Quaternary Science Reviews*, *241*, 106396. https://doi.org/10.1016/j.quascirev.2020.106396

Gebbie, G. (2014). How much did Glacial North Atlantic water shoal? *Paleoceanography*, *29*(3), 190–209. https://doi.org/10.1002/2013PA002557

Grousset, F. E., Cortijo, E., Huon, S., Herv, L., Richter, T., Burdloff, D., et al. (2001). Zooming in on Heinrich layers 1. *Paleoceanography*, *16*(3), 240–259. https://doi.org/10.1029/2000pa000559

Howe, J. N. W., & Piotrowski, A. M. (2017). Atlantic deep water provenance decoupled from atmospheric CO_2 concentration during the lukewarm interglacials. *Nature Communications*, *8*(1), 2003. https://doi.org/10.1038/s41467-017-01939-w

Howe, J. N. W., Piotrowski, A. M., Noble, T. L., Mulitza, S., Chiessi, C. M., & Bayon, G. (2016). North Atlantic deep water production during the last glacial maximum. *Nature Communications*, *7*, 11765. https://doi.org/10.1038/ncomms11765

Howe, J. N. W., Piotrowski, A. M., & Rennie, V. C. F. (2016). Abyssal origin for the early Holocene pulse of unradiogenic neodymium isotopes in Atlantic seawater. *Geology*, *44*(10), 831–834. https://doi.org/10.1130/G38155.1

Huang, H., Gutjahr, M., Eisenhauer, A., & Kuhn, G. (2020). No detectable Weddell Sea Antarctic bottom water export during the last and penultimate glacial maximum. *Nature Communications*, *11*, 424. https://doi.org/10.1038/s41467-020-14302-3

Jaccard, S. L., Galbraith, E. D., Martínez-Garciá, A., & Anderson, R. F. (2016). Covariation of deep Southern Ocean oxygenation and atmospheric CO_2 through the last ice age. *Nature*, *530*(7589), 207–210. https://doi.org/10.1038/nature16514

Jacobsen, S. B., & Wasserburg, G. J. (1980). Sm-Nd isotopic evolution of chondrites. *Earth and Planetary Science Letters*, *50*(1), 139–155. https://doi.org/10.1016/0012-821X(80)90125-9

Jaume-Seguí, M., Kim, J., Pena, L. D., Goldstein, S. L., Knudson, K. P., Yehudai, M., et al. (2020). Distinguishing glacial AMOC and interglacial non–AMOC Nd isotopic signals in the deep Western Atlantic over the last 1 Myr. *Paleoceanography and Paleoclimatology*, *36*, e2020PA003877. https://doi.org/10.1029/2020PA003877

Jenkins, W. J., Smethie, W. M., Boyle, E. A., & Cutter, G. A. (2015). Water mass analysis for the U.S. GEOTRACES (GA03) North Atlantic sections. *Deep-Sea Research Part II: Topical Studies in Oceanography*, *116*, 6–20. https://doi.org/10.1016/j.dsr2.2014.11.018

Lambelet, M., van de Flierdt, T., Crocket, K., Rehkämper, M., Kreissig, K., Coles, B., et al. (2016). Neodymium isotopic composition and concentration in the western North Atlantic Ocean: Results from the GEOTRACES GA02 section. *Geochimica et Cosmochimica Acta*, *177*, 1–29. https://doi.org/10.1016/j.gca.2015.12.019

Lang, D. C., Bailey, I., Wilson, P. A., Chalk, T. B., Foster, G. L., & Gutjahr, M. (2016). Incursions of southern-sourced water into the deep North Atlantic during late Pliocene glacial intensification. *Nature Geoscience*, *9*(5), 375–379. https://doi.org/10.1038/ngeo2688

Lippold, J., Gutjahr, M., Blaser, P., Christner, E., de Carvalho Ferreira, M. L., Mulitza, S., et al. (2016). Deep water provenance and dynamics of the (de)glacial Atlantic meridional overturning circulation. *Earth and Planetary Science Letters*, *445*, 68–78. https://doi.org/10.1016/j.epsl.2016.04.013

Lynch-Stieglitz, J., Adkins, J. F., Curry, W. B., Dokken, T., Hall, I. R., Herguera, J. C., et al. (2007). Atlantic meridional overturning circulation during the last glacial maximum. *Science*, *316*(5821), 66–69. https://doi.org/10.1126/science.1137127

Marchitto, T. M., & Broecker, W. S. (2006). Deep water mass geometry in the glacial Atlantic Ocean: A review of constraints from the paleonutrient proxy Cd/Ca. *Geochemistry, Geophysics, Geosystems*, *7*(12), Q12003. https://doi.org/10.1029/2006GC001323

McManus, J. F., Francois, R., Gherardl, J. M., Kelgwin, L., & Drown-Leger, S. (2004). Collapse and rapid resumption of Atlantic meridional circulation linked to deglacial climate changes. *Nature*, *428*(6985), 834–837. https://doi.org/10.1038/nature02494

Menviel, L., Timmermann, A., Friedrich, T., & England, M. H. (2014). Hindcasting the continuum of Dansgaard-Oeschger variability: Mechanisms, patterns and timing. *Climate of the Past*, *10*, 63–77. https://doi.org/10.5194/cp-10-63-2014

Naafs, B. D. A., Hefter, J., Grützner, J., & Stein, R. (2013). Warming of surface waters in the mid-latitude North Atlantic during Heinrich events. *Paleoceanography*, *28*(1), 153–163. https://doi.org/10.1029/2012PA002354

Oppo, D. W., Gebbie, G., Huang, K. F., Curry, W. B., Marchitto, T. M., & Pietro, K. R. (2018). Data constraints on glacial Atlantic water mass geometry and properties. *Paleoceanography and Paleoclimatology*, *33*(9), 1013–1034. https://doi.org/10.1029/2018PA003408

Petit, J. R., Jouzel, J., Raynaud, D., Barnola, J. M., Basile, I., Bender, M., et al. (1999). Climate and atmospheric history of the past 420,000 years from the Vostok ice core, Antarctica. *Nature*, *399*, 348–436. https://doi.org/10.1038/20859

Piotrowski, A. M., Goldstein, S. L., Hemming, S. R., & Fairbanks, R. G. (2004). Intensification and variability of ocean thermohaline circulation through the last deglaciation. *Earth and Planetary Science Letters*, *225*(1–2), 205–220. https://doi.org/10.1016/j.epsl.2004.06.002

Piotrowski, A. M., Goldstein, S. L., Hemming, S. R., & Fairbanks, R. G. (2005). Temporal relationships of carbon cycling and ocean circulation at glacial boundaries. *Science*, *307*(5717), 1933–1938. https://doi.org/10.1126/science.1104883

Pöppelmeier, F., Blaser, P., Gutjahr, M., Jaccard, S., Frank, M., Max, L., & Lippold, J. (2020). Northern sourced water dominated the Atlantic ocean during the last glacial maximum. *Geology*, *48*(8), 826–829. https://doi.org/10.1130/G47628.1

Pöppelmeier, F., Blaser, P., Gutjahr, M., Süfke, F., Thornalley, D. J. R., Grützner, J., et al. (2019). Influence of ocean circulation and benthic exchange on deep northwest Atlantic Nd isotope records during the past 30,000 years. *Geochemistry, Geophysics, Geosystems*, *20*(9), 4457–4469. https://doi.org/10.1029/2019GC008271

Pöppelmeier, F., Frank, N., Blaser, P., & Lippold, J. (2020). Authigenic neodymium isotope data from site M45/5_90 since the last glacial. *PANGAEA*. https://doi.org/10.1594/PANGAEA.925737

Pöppelmeier, F., Gutjahr, M., Blaser, P., Keigwin, L. D., & Lippold, J. (2018). Origin of Abyssal NW Atlantic water masses since the last glacial maximum. *Paleoceanography and Paleoclimatology*, *33*(5), 530–543. https://doi.org/10.1029/2017PA003290

Pöppelmeier, F., Scheen, J., Blaser, P., Lippold, J., Gutjahr, M., & Stocker, T. F. (2020). Influence of elevated Nd fluxes on the northern Nd isotope end-member of the Atlantic during the early Holocene. *Paleoceanography and Paleoclimatology*, *35*, e2020PA003973. https://doi.org/10.1029/2020PA003973

Rahlf, P., Hathorne, E., Laukert, G., Gutjahr, M., Weldeab, S., & Frank, M. (2020). Tracing water mass mixing and continental inputs in the southeastern Atlantic Ocean with dissolved neodymium isotopes. *Earth and Planetary Science Letters*, *530*, 115944. https://doi.org/10.1016/j.epsl.2019.115944

Rahmstorf, S. (2002). Ocean circulation and climate during the past 120,000 years. *Nature*, *419*(6903), 207–214. https://doi.org/10.1038/nature01090

Ruddiman, W. F., Raymo, M. E., Martinson, D. G., Backman, J., & Backman, J. (1989). Pleistocene evolution: Northern hemisphere ice sheets and North Atlantic Ocean. *Paleoceanography*, *4*(4), 353–412. https://doi.org/10.1029/PA004i004p00353

Simpson, G. L. (2018). Modelling palaeoecological time series using generalised additive models. *Frontiers in Ecology and Evolution*, *6*, 1–21. https://doi.org/10.3389/fevo.2018.00149

Skinner, L. C., Scrivner, A. E., Vance, D., Barker, S., Fallon, S., & Waelbroeck, C. (2013). North Atlantic versus Southern Ocean contributions to a deglacial surge in deep ocean ventilation. *Geology*, *41*(6), 667–670. https://doi.org/10.1130/G34133.1

Smith, M. E., Glick, E. V., Lodestro, S., & Rashid, H. (2013). Data report: Oxygen isotopes and foraminifer abundance record for the last glacial-interglacial cycle and marine isotope Stage 6 at IODP Site U1313. In *Procceedings of IODP*. Integrated Ocean Drilling Program Management International, Inc. https://doi.org/10.2204/iodp.proc.303306.216.2013

Stichel, T., Frank, M., Rickli, J., & Haley, B. A. (2012). The hafnium and neodymium isotope composition of seawater in the Atlantic sector of the Southern Ocean. *Earth and Planetary Science Letters*, *317–318*, 282–294. https://doi.org/10.1016/j.epsl.2011.11.025

Stichel, T., Hartman, A. E., Duggan, B., Goldstein, S. L., Scher, H., & Pahnke, K. (2015). Separating biogeochemical cycling of neodymium from water mass mixing in the Eastern North Atlantic. *Earth and Planetary Science Letters*, *412*, 245–260. https://doi.org/10.1016/j.epsl.2014.12.008

Tachikawa, K., Arsouze, T., Bayon, G., Bory, A., Colin, C., Dutay, J. C., et al. (2017). The large-scale evolution of neodymium isotopic composition in the global modern and Holocene ocean revealed from seawater and archive data. *Chemical Geology*, *457*, 131–148. https://doi.org/10.1016/j.chemgeo.2017.03.018

Tanaka, T., Togashi, S., Kamioka, H., Amakawa, H., Kagami, H., Hamamoto, T., et al. (2000). JNdi-1: A neodymium isotopic reference in consistency with LaJolla neodymium. *Chemical Geology*, *168*(3–4), 279–281. https://doi.org/10.1016/S0009-2541(00)00198-4

van de Flierdt, T., Grifths, A. M., Lambelet, M., Little, S. H., Stichel, T., & Wilson, D. J. (2016). Neodymium in the oceans: A global database, a regional comparison and implications for palaeoceanographic research. *Philosophical Transactions of the Royal Society A: Mathematical, Physical and Engineering Sciences*, *374*, 20150293. https://doi.org/10.1098/rsta.2015.0293

Zhao, N., Oppo, D. W., Huang, K. F., Howe, J. N. W., Blusztajn, J., & Keigwin, L. D. (2019). Glacial–interglacial Nd isotope variability of North Atlantic Deep Water modulated by North American ice sheet. *Nature Communications*, *10*(1), 1–10. https://doi.org/10.1038/s41467-019-13707-z

References From the Supporting Information

Bickert, T., Curry, W., & Wefer, G. (1997). Late Pliocene to Holocene (2.6-0 Ma) western equatorial Atlantic deep-water circulation: Inferences from benthic stable isotopes. *Proceedings of the Ocean Drilling Program, Scientific Results*, *154*, 239–254. https://doi.org/10.2973/odp.proc.sr.154.110.1997

Gutjahr, M., Frank, M., Stirling, C. H., Klemm, V., van de Flierdt, T., & Halliday, A. N. (2007). Reliable extraction of a deepwater trace metal isotope signal from Fe-Mn oxyhydroxide coatings of marine sediments. *Chemical Geology*, *242*(3–4), 351–370. https://doi.org/10.1016/j.chemgeo.2007.03.021

Lisiecki, L. E., & Stern, J. V. (2016). Regional and global benthic $\delta^{18}O$ stacks for the last glacial cycle. *Paleoceanography*, *31*, 1368–1394. https://doi.org/10.1002/2016PA003002